Multiple PET Reconstruction Assisted Non-local Mean Denoising of PET Images

Hossein Arabi and Habib Zaidi, *Fellow, IEEE*

***Abstract*– Non-local mean (NLM) denoising is commonly used for noise suppression in natural as well as medical imaging. Basically, the NLM filter takes advantage of the redundant information present in the image in the form of repeated structures/patterns to identify the underlying signals. In medical imaging (particularly PET and SPECT imaging), different representations of the image data under study (target or original image) could be reconstructed via applying different reconstruction settings. These representative (auxiliary) images bear very similar patterns/structures to the original/target image with different signal-to-noise ratios (SNR) which are ideal for use in the NLM denoising approach. This study proposed the multiple-reconstruction NLM filtering approach (referred to as MR-NLM) for noise reduction in PET imaging, wherein the redundant information present in auxiliary PET images are employed to conduct the NLM denoising process. The MR-NLM method relies on 12 additional PET image reconstructions (apart from the target PET image) using the same iterative algorithm with different iterations and subset numbers. Thereafter, for each target voxel, patches of voxels are extracted at the same location from all auxiliary PET images to be fed into the NLM smoothing process. To evaluate the performance of the MR-NLM algorithm, post-reconstruction denoising approaches including the conventional NLM, bilateral, and Gaussian filters were implemented and compared using 25 ^{18}F-FDG clinical whole-body (WB) PET/CT studies. The clinical studies demonstrated superior performance of the MR-NLM approach which established a promising compromise between noise suppression and preservation of the underlying signal/structures in PET images leading to higher SNR compared to the conventional NLM approach (34.9±5.7 versus 32.4±5.5). Though MR-NLM exhibited promising performance, this method suffers from long processing time due to the requirement of multiple reconstructions of raw PET data.**

***Index Terms*— PET/CT, non-local mean, noise, post-reconstruction filter.**

I. Introduction

POSITRON emission tomography (PET) scans normally bear relatively high noise levels, which would adversely affect their clinical value and might lead to misdiagnosis. Post-reconstruction denoising approaches may cause quantitative bias, signal loss, and image artifact [1].

Manuscript was submitted December 20, 2020. This work was supported by the Swiss National Science Foundation under grant SNRF 320030_176052 and the Private Foundation of Geneva University Hospitals under Grant RC-06-01.

H. Arabi and H. Zaidi are with the Division of Nuclear Medicine & Molecular Imaging, Geneva University Hospital, Geneva, Switzerland (e-mail: hossein.arabi@unige.ch, habib.zaidi@hcuge.ch).

To address these issues, the edge-preserving noise suppression methods have been proposed to maintain the prominent signals/edges while suppressing the noise in an attempt to maximize the signal-to-noise-ratio (SNR) in SPECT [2] and PET images [3].

Among the edge-preserving denoising techniques, the non-local mean approach (NLM) [4] has shown an excellent capability to enhance the SNR in PET images through effective noise reduction while maintaining the underlying structures/patterns [5]. The NLM denoising approach explores the target image (normally within a predefined search window) to find similar structures and repeated patterns in order to distinguish the noise from the underlying signals and/or structures. The performance of the NLM filter greatly depends on the search scheme and the similarity of the extracted non-local patches/patterns.

This work proposed a dedicated NLM smoothing approach (in other words, a novel patch search scheme) for the SPECT and PET images. The proposed NLM denoising approach takes the advantage of the fact that raw data from PET or SPECT imaging could be reconstructed multiple times using different reconstruction algorithms or settings. These auxiliary PET or SPECT images, reconstructed from the same raw data, contain almost the same patterns, structures, and textures to the original/target image. However, the noise levels or the signal to background convergence would be different among them. In this light, these auxiliary images will provide highly similar patches with the same underlying structures/patterns to be fed into the NLM denoising approach to suppress the noise in the target images [6].

This work investigates the feasibility of conducting the multiple reconstruction-guided NLM denoising (so-called MR-NLM) on the whole-body PET images through employing the patches of voxels extracted from a number of PET images reconstructed from the same raw PET data.

II. Materials and Methods

Multiple-reconstruction non-local mean (MR-NLM) filter

The conventional NLM filter relies on similar textures and structures within the target images to extract similar patches of voxels to suppress the noise in the target patch via calculating the weighted average of the extracted patches. The conventional NLM seeks to find similar patches of voxels within the sub-volume of the target image which is normally determined by the user as the search window (Fig 1A). The performance of the NLM denoising approaches highly depends on the similarity of the extracted patches (in terms of underlying structures). Multiple reconstructions of the raw PET data with different image reconstruction settings would readily offer very similar patches of voxels at the same

2020 IEEE Nuclear Science Symposium and Medical Imaging Conference (NSS/MIC) | 978-1-7281-7693-2/20/$31.00 ©2020 IEEE | DOI: 10.1109/NSS/MIC42677.2020.9507772

978-1-7281-7693-2/20/$31.00 ©2020 IEEE

spatial location. These auxiliary PET images (reconstructed with slightly different settings) contain very similar signals and structures contaminated with different noise levels or may present different signal to background (convergence) ratio. The extracted patches from these auxiliary PET images would supply the NLM filter with ideal similar patches to conduct the denoising process in the target image (Fig 1B). In the proposed MR-NLM approach, the search window used in the conventional NLM filter (blue square in Fig. 1A) is no longer needed and instead, the similar patches extracted from the auxiliary images are used to estimate a noise-free patch (via calculating the weighted average of the extracted patches together with the target patch) for the target voxel in the original image. In this procedure, each auxiliary image provides only a single patch at the same spatial location.

Algorithmic implementation

The target PET images were reconstructed using the conventional TOF/PSF OP-OSEM (time-of-flight/point spread function ordinary Poisson ordered subset-expectation maximization) algorithm with 2 iterations and 21 subsets. To generate auxiliary PET images, the same reconstruction algorithm (TOF/PSF OP-OSEM) was employed but with different numbers of iterations and subsets to generate auxiliary PET images. 12 iteration/subset pairs were selected in such a way to lead to similar convergence (signal to background ratio) and noise levels to the target PET images. The estimated noise levels in the liver and the lesion to liver uptake ratio in 8 clinical PET/CT studies were examined to select these 12 pairs indicated in Fig. 2.

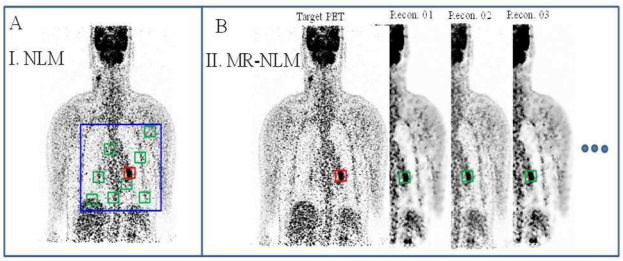

Fig. 1. A) Conventional NLM filter with the indicated search window (blue box), target patch (red box), and similar patches (green boxes) found within the search window. B) Multiple-reconstruction NLM filter (MR-NLM) with the indicated target patch (red box) and the same patches of voxels defined on the auxiliary PET images at the same spatial location. constructions of the PET data.

Clinical evaluation

The MR-NLM approach was evaluated against the conventional NLM, bilateral filter, and commonly used Gaussian post-reconstruction denoising methods through the calculation of the SNR (Eq. 1) and quantitative bias (%) (Eq. 2) on 50 volumes of interest (VOI) manually defined on malignant lesions.

$$SNR = \frac{1}{Ns}\sum_{k=1}^{Ns}\frac{(\mu_{target(k)} - \mu_{bg(k)})}{\sigma_k} \quad (1)$$

$$Bias(\%) = 100 \times \frac{\mu_{target} - \mu_{noisy}}{\mu_{noisy}} \quad (2)$$

μ_{target} and μ_{bg} denote the mean values of the voxel intensities in the target and background VOIs. σ_k indicates the standard deviation measured within the background. μ_{noisy} denotes the average of the activity concentration within the VOIs drawn on the original (before denoising) PET images (referred to as OSEM).

III. Results and Discussion

Fig. 3 illustrates the transaxial views of a whole-body PET scan before and after application of the Gaussian, bilateral, conventional NLM, and MR-NLM filters. The patient in Fig. 3 presents a non-small lung cancer, wherein the vertical line profiles plotted over the lesion compare the performance of the different denoising approaches. Visual inspection of the Gaussian filtered images revealed over-smoothed patterns/structures compared to the outcomes of the NLM and MR-NLM filters with noticeably less signal loss and/or quantitative bias. Regarding, the bias maps obtained from subtraction of the filtered images from the original noisy image (OSEM), the MR-NLM filter resulted in smallest over-smoothed structures and signal loss, in particular over the malignant lesion in the lung.

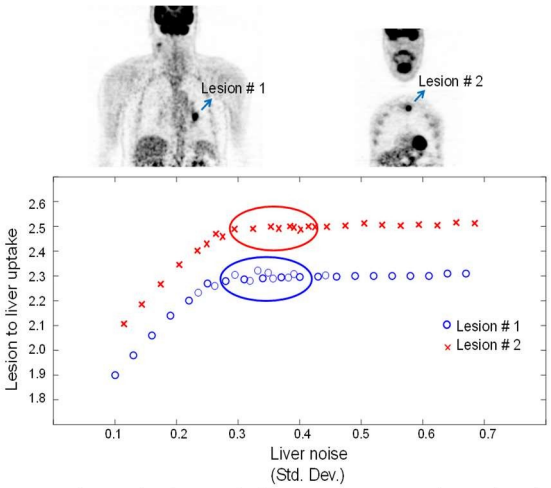

Fig. 2. Lesion to background (liver) contrast (uptake) ratio plotted against the noise (standard deviation) in the background (liver) for two malignant lesions (two different patients) in the whole-body PET/CT images. The circles and crosses indicate the different reconstructions of the same raw PET data using different iteration/subsets numbers. The following iteration and subset numbers were used for the implementation of the MR-NLM filter: 2i:24s, 3i:14s, 3i:21s, 4i:8s, 2i:28s, 3i:12s, 4i:12s, 7i:6s, 5i:8s, 6i:7s, 5i:7s, and 5i:6s. The original (target) PET image was reconstructed with 2 iterations and 21 subsets (2i:21s).

The results of the quantitative analysis of the different denoising techniques on the ^{18}F-FDG PET whole-body scans are presented in Table 1. The proposed MR-NLM method resulted in an SNR and bias of 34.9±5.7 and -2.2±1.2% measured over the 50 VOIs drawn on the malignant lesions (hot spots). The conventional NLM filter exhibited inferior performance leading to an SNR and bias of 32.4±5.5 and -3.5±1.3%, respectively, with a statistically significant difference (p-value<0.02) with the MR-NLM approach.

The idea proposed in this work (employing various image reconstructions of the same PET raw data to create different representations of the PET information/signals) could be exploited in a deep learning framework [7] to estimate high quality or standard PET images from fast or low dose scans [8-10].

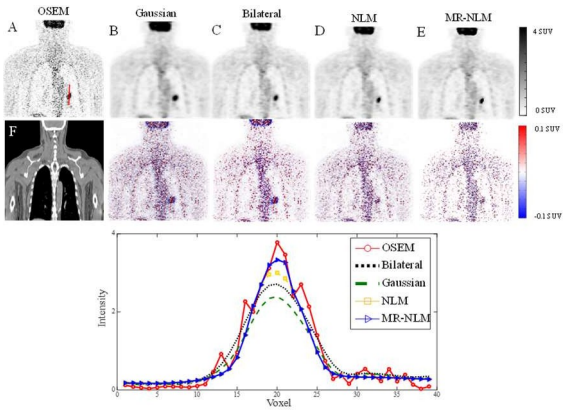

Fig. 3. Sagittal views of the PET scan of a representative patient bearing a non-small lung cancer together with the corresponding CT image. A) Original PET image before denoising (OSEM) and the filtered PET images and using B) Gaussian, C) bilateral, D) conventional NLM and E) proposed MR-NLM denoising approaches. The corresponding bias maps obtained from filtered - OSEM are also presented below the PET images. F) CT image. The bottom panel present the vertical line profiles drawn on the PET images before and after the application of the different denoisingtechniques over the malignant lesion.

TABLE 1. MEAN SUV BIAS AND SNR (±STANDARD DEVIATION) MEASURED OVER 50 VOIS DRAWN OVER THE MALIGNANT LESIONS (HOT SPOTS). THE ORIGINAL NOISY IMAGES (OSEM) WERE CONSIDERED AS THE REFERENCE FOR THE CALCULATION OF THE SUV BIAS.

	SNR	**Lesion SUV_{mean}**	**Bias (%)**
OSEM	23.3±6.8	7.8±2.0	-
Gaussian	26.5±5.5	6.6±1.9	-12.3±2.3
Bilateral	29.2±5.9	6.8±1.9	-7.7±2.1
NLM	32.4±5.5	7.1±1.7	-3.5±1.3
MR-NLM	34.9±5.7	7.3±1.6	-2.2±1.2
***p*-value**	0.02	0.03	0.02

IV. Conclusion

The clinical evaluation of the proposed MR-NLM denoising technique revealed its superior performance in terms of effective noise reduction as well as preserving the underlying structures and signals in whole-body PET scans compared to the conventional NLM approach. Though the MR-NLM exhibited promising performance, the implementation of this technique imposes high computational time due to multiple PET image reconstruction.

References

[1] H. Arabi and H. Zaidi, "Spatially guided nonlocal mean approach for denoising of PET images," *Med Phys,* vol. 47, no. 4, pp. 1656-1669, Apr 2020.

[2] N. Zeraatkar *et al.*, "Resolution-recovery-embedded image reconstruction for a high-resolution animal SPECT system," *Phys Med,* vol. 30, no. 7, pp. 774-81, Nov 2014.

[3] H. Arabi and H. Zaidi, "Improvement of image quality in PET using post-reconstruction hybrid spatial-frequency domain filtering," *Phys Med Biol,* vol. 63, no. 21, p. 215010, Oct 24 2018.

[4] A. Buades, B. Coll, and J.-M. Morel, "A non-local algorithm for image denoising," in *2005 IEEE Computer Society Conference on Computer Vision and Pattern Recognition (CVPR'05)*, 2005, vol. 2, pp. 60-65: IEEE.

[5] C. Chan, R. Fulton, R. Barnett, D. D. Feng, and S. Meikle, "Post-reconstruction nonlocal means filtering of whole-body PET with an anatomical prior," *IEEE Trans Med Imaging,* vol. 33, no.3, pp. 636-50, Mar 2014.

[6] H. Arabi and H. Zaidi, "Non-local mean denoising using multiple PET reconstructions," *Ann Nucl Med,* Nov 26 2020.

[7] H. Arabi and H. Zaidi, "Applications of artificial intelligence and deep learning in molecular imaging and radiotherapy," *Eur. J. Hybrid Imaging,* vol. 4, no. 1, p. 17, 2020/09/23.

[8] A. Sanaat, H. Arabi, I. Mainta, V. Garibotto, and H. Zaidi, "Projection Space Implementation of Deep Learning-Guided Low-Dose Brain PET Imaging Improves Performance over Implementation in Image Space," *J Nucl Med,* vol. 61, no. 9, pp. 1388-1396, Sep 2020.

[9] B. Sanaei, R. Faghihi, and H. Arabi, "Quantitative investigation of low-dose PET imaging and post-reconstruction smoothing," *arXiv* preprint arXiv:2103.10541, 2021.

[10] N. A. Olia et al., "Deep learning-based noise reduction in low dose SPECT Myocardial Perfusion Imaging: Quantitative assessment and clinical performance," *arXiv* preprint arXiv:2103.11974, 2021.